

**Effect of nonhydrostatic stresses on solid-fluid equilibrium. I. Bulk thermodynamics**

T. Frolov\* and Y. Mishin†

*Department of Physics and Astronomy, George Mason University, MSN 3F3, Fairfax, Virginia 22030, USA*

(Received 26 July 2010; published 16 November 2010)

We present a thermodynamic analysis of the effect of nonhydrostatic stresses on solid-fluid equilibrium in single-component systems. The solid is treated in the small-strain approximation and anisotropic linear elasticity. If the latent heat of the solid-fluid transformation is nonzero and pressure in the fluid is fixed, the shift of the equilibrium temperature relative to hydrostatic equilibrium is shown to be quadratic in nonhydrostatic components of the stress. If atomic volumes of the phases are different and temperature is fixed, the shift of the equilibrium liquid pressure relative to a hydrostatic state is quadratic in nonhydrostatic components of the stress in the solid. The stress effects at special points, at which either the latent heat or the volume difference turn to zero, have also been analyzed. Our theoretical predictions for the temperature and pressure shifts are quantitatively verified by atomistic computer simulations of solid-liquid equilibrium in copper using molecular dynamics with an embedded-atom potential. The simulations also demonstrate spontaneous crystallization of liquid on the surface of a stressed solid with the formation of solid-solid interfaces with the same crystallographic orientation of the solid layers. The lattice mismatch between the stressed and unstressed regions is accommodated by misfit dislocations dissociated in a zigzag pattern.

DOI: [10.1103/PhysRevB.82.174113](https://doi.org/10.1103/PhysRevB.82.174113)

PACS number(s): 62.50.-p, 64.70.dm, 67.80.bf

**I. INTRODUCTION**

The problem of equilibrium between nonhydrostatically stressed solids and fluids is relevant to many processes encountered in nature and technological applications. For example, crystallization of solid materials may occur in the presence of pressure in the liquid. The pressure gives rise to mechanical stresses in the growing solid, which are generally not hydrostatic. As another example, during deposition of thin solid films by growth from vapor, the films are often subject to nonhydrostatic stresses imposed by the substrate, especially during epitaxial growth. In a more general context, nonhydrostatic stresses can strongly affect phase stability and phase transformations and are very important in high-pressure physics.<sup>1</sup>

Equilibrium between nonhydrostatically stressed solids and fluids was first discussed by Gibbs.<sup>2</sup> He derived equilibrium conditions between the phases and showed that a nonhydrostatic single-component solid<sup>3</sup> can be equilibrated with three separate multicomponent fluids each having a different chemical potential. Gibbs also showed that a multicomponent fluid equilibrated with a single-component solid is supersaturated with respect to the substance of the solid except when the solid is hydrostatic. He pointed out that for variations in stress away from the hydrostatic state at a constant pressure  $p$  in the fluid, the change in the equilibrium temperature  $T$  is zero to first order. Using isotropic linear elasticity, Seckerka and Cahn<sup>4</sup> recently showed that the change in equilibrium temperature in a single-component system at a fixed pressure in the fluid is quadratic in nonhydrostatic components of the stress in the solid.

In this work we analyze general variations in state of an equilibrium solid-fluid system. We evaluate the changes in  $T$  and  $p$  caused by stress variations away from an initially hydrostatic state along a hydrostatic path, as well as along nonhydrostatic isobaric and isothermal paths. Our treatment includes analysis of special points where volumes per atom or

entropy per atom in the initial hydrostatic state are the same in both phases. We treat the elastic deformations of the solid within a small-strain approximation and anisotropic linear elasticity. Using atomistic simulations with a semiempirical potential, we study nonhydrostatic solid-liquid equilibrium in pure copper with a (110)-oriented interface. As most crystalline solids, copper is elastically anisotropic. Using molecular dynamics (MD), we directly compute several equilibrium temperatures at a fixed zero pressure in the liquid and several equilibrium pressures at a constant temperature. The calculations are performed for a set of different states of stress in the solid, including biaxial deformations. The results are compared with our theoretical predictions and are found to be in quantitative agreement. We also study the instability of nonhydrostatic systems predicted by Gibbs and show how a nonhydrostatic system can transform to hydrostatic by growth of hydrostatically stressed solid layers.

The paper is organized as follows. In Sec. II we analyze thermodynamic relations for nonhydrostatic solid-fluid equilibrium and derive analytical expressions for the equilibrium temperature and pressure. In Sec. III we describe our methodology of atomistic simulations. The results of the simulations are presented in Sec. IV, followed by a discussion in Sec. V. The results obtained in this paper will be used for the analysis of solid-fluid interface thermodynamics in Part II of this work.<sup>5</sup>

**II. THERMODYNAMICS OF NONHYDROSTATIC SOLID-FLUID EQUILIBRIUM****A. Thermodynamic relations**

Consider a rectangular block containing a single-component homogeneous solid under a general state of mechanical stress at equilibrium with a fluid of the same component. The phases are separated by a planar interface and the effect of gravity<sup>6,7</sup> is neglected. Gibbs derived the follow-

ing equilibrium conditions for this system: (1) temperature  $T$  is uniform throughout the system; (2) one of the principal axes of the Cauchy stress tensor  $\sigma_{ij}$  in the solid (call it axis 3) is perpendicular to the solid-fluid interface with the principal value  $\sigma_{33} = -p$ , where  $p$  is pressure in the fluid; and (3) the phase-change equilibrium condition requires

$$u^s - Ts^s + p\Omega^s = \mu^f. \quad (1)$$

Here  $u^s$ ,  $s^s$ , and  $\Omega^s$  are the energy, entropy, and volume per atom in the solid and  $\mu^f$  is the chemical potential in the fluid.

For a general variation in the state of stress and the entropy of the solid, the differential of  $u^s$  is given by the fundamental equation

$$du^s = Tds^s + \sum_{i,j=1,2,3} \Omega_0^s \sigma_{ij} de_{ij}, \quad (2)$$

where  $e_{ij}$  is the small-strain tensor and  $\Omega_0^s$  is atomic volume in the reference state used to define the strain. As the reference state we choose the stress-free state of the solid at a fixed reference temperature  $T_0$ . The differential of the chemical potential in the fluid is given by

$$d\mu^f = -s^f dT + \Omega^f dp, \quad (3)$$

where  $s^f$  and  $\Omega^f$  are entropy and volume per atom in the fluid. Taking a differential of Eq. (1) and using Eqs. (2) and (3) in conjunction with the relation

$$d\Omega^s = \sum_{i,j=1,2,3} \Omega_0^s \delta_{ij} de_{ij} \quad (4)$$

( $\delta_{ij}$  being the Kronecker symbol) we obtain

$$\Delta s dT - \Delta \Omega dp + \sum_{i,j=1,2} \Omega_0^s (\sigma_{ij} + \delta_{ij} p) de_{ij} = 0, \quad (5)$$

where we denoted  $\Delta s = s^f - s^s$  and  $\Delta \Omega = \Omega^f - \Omega^s$ . Note that the summation now extends only to  $i, j = 1, 2$  because  $\sigma_{3k} + \delta_{3k} p = 0$  for  $k = 1, 2, 3$ . Gibbs derived Eq. (5) for a more general case of finite strains.<sup>2</sup> This equation contains five differentials and defines a four-dimensional (4D) phase coexistence surface in the five-dimensional (5D) configuration space of variables. Thus the system has four degrees of freedom (four independent variables).

Equation (5) immediately leads to two important conclusions regarding the behavior of  $T$  and  $p$  on the phase coexistence surface. If Eq. (5) is applied to a variation away from a hydrostatic state, the coefficients  $\sigma_{ij} + \delta_{ij} p$  vanish. Then, if  $\Delta s$  in the hydrostatic state is finite and the solid is deformed elastically at a constant pressure in the fluid, the change in temperature is zero to first order:  $dT = 0$ . Similarly, if  $\Delta \Omega$  in the hydrostatic state is finite and temperature is constant, the change in pressure due to elastic strains is zero to the first order:  $dp = 0$ .

To make further progress in this analysis, additional approximations have to be made. Specifically, we will adopt the approximation of anisotropic linear elasticity, in which the strain and stress tensors are related by

$$e_{ij} = \sum_{k,l=1,2,3} S_{ijkl} \sigma_{kl} + \eta_{ij}. \quad (6)$$

Here  $S_{ijkl}$  is the tensor of isothermal compliances, which we assume to be constant.  $\eta_{ij}$  is a tensor function of  $T - T_0$ , where  $T_0$  is the chosen reference temperature. This tensor represents the contribution to strain due to thermal expansion of the stress-free solid. If  $\eta_{ij}$  is approximated by a linear function of  $T - T_0$ , Eq. (6) becomes the Duhamel-Neumann form of Hooke's law.<sup>8</sup>

Inserting Eq. (6) in Eq. (5) and denoting the nonhydrostatic components of the stress by  $q_{ij} = \sigma_{ij} + \delta_{ij} p$ , we obtain

$$\begin{aligned} (\Delta s + \Omega_0^s q_{ij} \eta'_{ij}) dT - \left( \Delta \Omega + \Omega_0^s \sum_{i,j,k,l=1,2,3} q_{ij} S_{ijkl} \delta_{kl} \right) dp \\ + \Omega_0^s \sum_{i,j,k,l=1,2} S_{ijkl} q_{ij} dq_{kl} = 0, \end{aligned} \quad (7)$$

where  $\eta'_{ij}$  is the temperature derivative of  $\eta_{ij}$  representing the thermal-expansion tensor. Although the summation in the differential coefficient before  $dp$  goes from 1 to 3, some of the terms are zero because  $q_{i3} = 0$ .

Some of the quantities appearing in the differential coefficients of Eq. (7) are related to each other. Using the Maxwell relations derived in Appendix A, it can be shown that the following differential equations must be satisfied:

$$\frac{\partial s^s}{\partial q_{ij}} = \Omega_0^s \eta'_{ij}, \quad i, j = 1, 2, \quad (8)$$

$$\frac{\partial \Omega^s}{\partial q_{ij}} = \Omega_0^s \sum_{k=1,2,3} S_{ijkk}, \quad i, j = 1, 2, \quad (9)$$

$$\frac{\partial \Omega^s}{\partial T} = - \frac{\partial s^s}{\partial p}, \quad (10)$$

$$\frac{\partial \Omega^f}{\partial T} = - \frac{\partial s^f}{\partial p}. \quad (11)$$

These equations will be used at the next step of the calculations.

Suppose the solid-fluid system is initially in an equilibrium state, denoted  $H$ , in which the solid is hydrostatic ( $q_{ij} = 0$ ) and the temperature and pressure are  $T_H$  and  $p_H$ , respectively. Our goal is to integrate Eq. (7) from state  $H$  to other (generally, nonhydrostatic) equilibrium states in a small vicinity of  $H$ . The integration will involve a linearization of the differential coefficients of  $dT$  and  $dp$ . To this end, we expand  $s^f$ ,  $s^s$ ,  $\Omega^f$ , and  $\Omega^s$  in Taylor series in the variables  $T - T_H$ ,  $p - p_H$ , and  $q_{ij}$  and limit the expansions to linear terms

$$s^f = \bar{s}^f + \left( \frac{\partial s^f}{\partial T} \right)_H (T - T_H) + \left( \frac{\partial s^f}{\partial p} \right)_H (p - p_H), \quad (12)$$

$$\begin{aligned} s^s = \bar{s}^s + \left( \frac{\partial s^s}{\partial T} \right)_H (T - T_H) + \left( \frac{\partial s^s}{\partial p} \right)_H (p - p_H) \\ + \sum_{i,j=1,2} \left( \frac{\partial s^s}{\partial q_{ij}} \right)_H q_{ij}, \end{aligned} \quad (13)$$

$$\Omega^f = \bar{\Omega}^f + \left( \frac{\partial \Omega^f}{\partial T} \right)_H (T - T_H) + \left( \frac{\partial \Omega^f}{\partial p} \right)_H (p - p_H), \quad (14)$$

$$\begin{aligned} \Omega^s = & \bar{\Omega}^s + \left( \frac{\partial \Omega^s}{\partial T} \right)_H (T - T_H) + \left( \frac{\partial \Omega^s}{\partial p} \right)_H (p - p_H) \\ & + \sum_{i,j=1,2} \left( \frac{\partial \Omega^s}{\partial q_{ij}} \right)_H q_{ij}. \end{aligned} \quad (15)$$

The quantities  $\bar{s}^f$ ,  $\bar{s}^s$ ,  $\bar{\Omega}^f$ , and  $\bar{\Omega}^s$  are properties of the initial hydrostatic state and subscript  $H$  emphasizes that the derivatives are evaluated at that state. The derivatives  $(\partial s^f / \partial T)_H$ ,  $(\partial s^s / \partial T)_H$ ,  $(\partial \Omega^f / \partial p)_H$ ,  $(\partial \Omega^s / \partial p)_H$ ,  $(\partial \Omega^f / \partial T)_H$ , and  $(\partial \Omega^s / \partial T)_H$  correspond to variations from state  $H$  along hydrostatic paths and are related to the heat capacities, compressibilities, and thermal expansions of the phases. By contrast, the derivatives  $(\partial s^s / \partial q_{ij})_H$  and  $(\partial \Omega^s / \partial q_{ij})_H$  correspond to nonhydrostatic variations in the solid away from state  $H$ . No  $q_{ij}$  terms appear in the expansions for  $s^f$  and  $\Omega^f$  because the fluid is incapable of nonhydrostatic variations.

Substituting expansions Eqs. (12)–(15) in Eq. (7) and using relations in Eqs. (8)–(11) we obtain

$$\begin{aligned} & \left[ \Delta \bar{s} + \left( \frac{\partial \Delta s}{\partial T} \right)_H (T - T_H) - \left( \frac{\partial \Delta \Omega}{\partial T} \right)_H (p - p_H) \right] dT \\ & - \left[ \Delta \bar{\Omega} + \left( \frac{\partial \Delta \Omega}{\partial T} \right)_H (T - T_H) + \left( \frac{\partial \Delta \Omega}{\partial p} \right)_H (p - p_H) \right] dp \\ & + \Omega_0^s \sum_{i,j,k,l=1,2} S_{ijkl} q_{ij} dq_{kl} = 0. \end{aligned} \quad (16)$$

We can now integrate Eq. (16) from the hydrostatic state  $H$  to a new state with  $T$ ,  $p$ , and  $q_{ij}$  to obtain

$$\begin{aligned} \Delta \bar{s}(T - T_H) + \frac{1}{2} \left( \frac{\partial \Delta s}{\partial T} \right)_H (T - T_H)^2 - \Delta \bar{\Omega}(p - p_H) \\ - \frac{1}{2} \left( \frac{\partial \Delta \Omega}{\partial p} \right)_H (p - p_H)^2 - \left( \frac{\partial \Delta \Omega}{\partial T} \right)_H (T - T_H)(p - p_H) \\ + \frac{\Omega_0^s}{2} \sum_{i,j,k,l=1,2} S_{ijkl} q_{ij} q_{kl} = 0. \end{aligned} \quad (17)$$

Mathematically, this equation defines a 4D quadric surface representing two-phase equilibrium states in the 5D configuration space of the variables  $T$ ,  $p$ ,  $q_{11}$ ,  $q_{12}$ , and  $q_{22}$ .

Equation (17) is the central result of our thermodynamic analysis of solid-fluid equilibrium. This equation permits predictions of temperature-pressure-stress relations for equilibrium processes in which the two-phase system deviates from a given hydrostatic state  $H$  along hydrostatic or nonhydrostatic paths. This equation is also valid for processes whose path is confined to a small vicinity of point  $H$  but does not necessarily go through this point. Below we will analyze three particular paths on the 4D coexistence surface: hydrostatic, isobaric, and isothermal. Yet another path will be discussed separately in Sec. II B.

### 1. Hydrostatic path

The solid-fluid system is initially in the hydrostatic state  $H$ . Consider a process in which  $p$  and  $T$  vary but the solid phase remains hydrostatic, i.e., all  $q_{ij}$  remain zero. Since three variables are fixed, the system has only one degree of freedom. Equation (17) becomes

$$\begin{aligned} \Delta \bar{s}(T - T_H) + \frac{1}{2} \left( \frac{\partial \Delta s}{\partial T} \right)_H (T - T_H)^2 - \Delta \bar{\Omega}(p - p_H) \\ - \frac{1}{2} \left( \frac{\partial \Delta \Omega}{\partial p} \right)_H (p - p_H)^2 - \left( \frac{\partial \Delta \Omega}{\partial T} \right)_H (T - T_H)(p - p_H) = 0. \end{aligned} \quad (18)$$

Suppose  $\Delta \bar{s}$  and  $\Delta \bar{\Omega}$  are nonzero, i.e., state  $H$  is not a special point. Then in a small enough vicinity of this state the second-order terms can be neglected and Eq. (18) reduces to

$$\Delta \bar{s}(T - T_H) = \Delta \bar{\Omega}(p - p_H). \quad (19)$$

As expected, this is an integrated form of the Clapeyron-Clausius equation for hydrostatic phases. This equation is often written in the form

$$\Delta \bar{h}(T - T_H) = \Delta \bar{\Omega} T_H (p - p_H), \quad (20)$$

where  $\Delta \bar{h} \equiv \Delta \bar{s} / T_H$  is the latent heat of the hydrostatic solid-fluid transformation. The latter is experimentally more readily accessible than  $\Delta \bar{s}$ .

A special case arises when  $\Delta \bar{s} = 0$  (and thus  $\Delta \bar{h} = 0$ ) but  $\Delta \bar{\Omega} \neq 0$ . At this point the equilibrium pressure is an extremum as a function of temperature.  $^3\text{He}$  is an example of a system exhibiting this type of behavior.<sup>9,10</sup> Keeping the term with  $(T - T_H)^2$  and  $(p - p_H)$  and neglecting higher-order terms, Eq. (18) gives the parabolic equilibrium curve

$$p - p_H = \frac{1}{2 \Delta \bar{\Omega}} \left( \frac{\partial \Delta s}{\partial T} \right)_H (T - T_H)^2. \quad (21)$$

For  $^3\text{He}$   $\Delta s$  is negative below  $T_H$  and positive above  $T_H$  whereas  $\Delta \bar{\Omega}$  remains positive. This produces a minimum of the melting pressure at  $T_H$ .<sup>9,10</sup>

In another special case  $\Delta \bar{\Omega} = 0$  but  $\Delta \bar{s} \neq 0$ . The equilibrium temperature is an extremum as a function of pressure. Retaining the terms with  $(T - T_H)$  and  $(p - p_H)^2$  and neglecting all other terms, the phase coexistence equation is again parabolic,

$$T - T_H = \frac{T_H}{2 \Delta \bar{h}} \left( \frac{\partial \Delta \Omega}{\partial p} \right)_H (p - p_H)^2. \quad (22)$$

For melting,  $\Delta \bar{h}$  is usually positive while  $\Delta \Omega$  is likely to decrease with pressure due to larger compressibility of the liquid phase. In such cases the melting temperature reaches a maximum at a certain pressure, as observed experimentally and in simulations for several materials.<sup>11–14</sup>

### 2. Isobaric path

In the second type of variation, the pressure in the fluid is fixed while the solid is subject to a nonhydrostatic stress. The

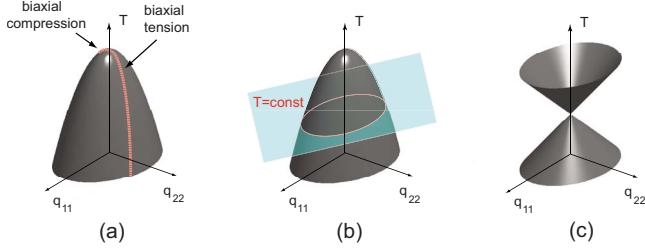


FIG. 1. (Color online) Schematic illustration of solid-fluid coexistence surfaces at constant pressure  $p$  in the fluid and  $q_{12}=0$  in the solid. The equilibrium temperature  $T$  is plotted as a function of two remaining nonhydrostatic components of the stress in the solid. (a) Path of biaxial tension and compression on the coexistence surface. (b) Isofluid path obtained by intersection of the paraboloid with an isothermal plane. (c) Phase coexistence surface when the initial hydrostatic state is a special point. If  $q_{12} \neq 0$ , the coexistence surfaces shown here become 3D and are difficult to visualize, but they remain paraboloids in (a) and (b) and an ellipsoidal double cone in (c).

system has three degrees of freedom and Eq. (17) reduces to

$$\Delta\bar{s}(T-T_H) + \frac{1}{2} \left( \frac{\partial\Delta s}{\partial T} \right)_H (T-T_H)^2 + \frac{\Omega_0^s}{2} \sum_{i,j=1,2} S_{ijkl} q_{ij} q_{kl} = 0. \quad (23)$$

If the  $\Delta\bar{s}$  is finite and the second term can be neglected in a given temperature range, we obtain

$$T-T_H = - \frac{\Omega_0^s T_H}{2\Delta\bar{h}} \sum_{i,j=1,2} S_{ijkl} q_{ij} q_{kl}. \quad (24)$$

Thus the temperature change is quadratic in nonhydrostatic stresses. The equilibrium surface is a three-dimensional (3D) paraboloid in the coordinates  $T$ ,  $q_{11}$ ,  $q_{12}$ , and  $q_{22}$  [see Figs. 1(a) and 1(b) for a particular case when  $q_{12}=0$  and the surface is a two-dimensional (2D) paraboloid]. Equation (24) generalizes the Sekerka and Cahn<sup>4</sup> result which was derived for an elastically isotropic solid. The quadratic form on the right-hand side of Eq. (24) is positive definite because it can be formally identified with work of elastic straining from a stress-free state to a state with  $\sigma_{ij}=q_{ij}$ , which is always positive for a stable crystal. Thus, if  $\Delta\bar{h}$  is positive (as it usually is for melting), then the equilibrium temperature decreases under nonhydrostatic stresses regardless of their sign.

For some cases it is advantageous to reformulate Eq. (24) in terms of strains instead of stresses. An expression for the equilibrium temperature as a function of lateral components of the strain tensor is derived in Appendix B. The strain formulation will be used in Part II of this work.<sup>5</sup>

Combining Eqs. (3) and (24) we can evaluate the change in the chemical potential  $\mu^f$  in the fluid due to deviation from hydrostatic equilibrium along a path defined by solid-fluid coexistence at a constant  $p$

$$\mu^f(T, p_H) - \mu^f(T_H, p_H) = \frac{\bar{s}^f \Omega_0^s T_H}{2\Delta\bar{h}} \sum_{i,j,k,l=1,2} S_{ijkl} q_{ij} q_{kl}. \quad (25)$$

To evaluate the stability of the fluid with respect to crystallization,  $\mu^f$  should be compared with the chemical potential,  $\mu_*^s$ , of a hydrostatic solid at the same temperature and the same pressure. The latter can be evaluated by

$$\mu_*^s(T, p_H) = \mu^f(T_H, p_H) - \bar{s}^s (T - T_H). \quad (26)$$

Thus,

$$\mu^f(T, p_H) - \mu_*^s(T, p_H) = -\Delta\bar{s}(T - T_H) = \frac{\Omega_0^s}{2} \sum_{i,j=1,2} S_{ijkl} q_{ij} q_{kl}, \quad (27)$$

where we used Eq. (24). Because this difference is positive, the fluid equilibrated with a nonhydrostatic solid is unstable with respect to crystallization to a hydrostatic solid.

If the initial hydrostatic state is a special point with  $\Delta\bar{s}=0$ , then we keep the quadratic term in Eq. (23) to obtain

$$(T - T_H)^2 = - \frac{\Omega_0^s}{\left( \frac{\partial\Delta s}{\partial T} \right)_H} \sum_{i,j,k,l=1,2} S_{ijkl} q_{ij} q_{kl}. \quad (28)$$

Recall that the quadratic form  $\sum S_{ijkl} q_{ij} q_{kl}$  is positive definite. Therefore, if  $(\partial\Delta s / \partial T)_H > 0$  as in the case of <sup>3</sup>He melting,<sup>10</sup> the only solution of this equation is  $T=T_H$  and  $q_{ij}=0$ . Thus, any infinitely small nonhydrostatic stress applied at constant  $p$  destroys the phase equilibrium. But if  $(\partial\Delta s / \partial T)_H < 0$ , then Eq. (28) has two solutions with opposite signs of  $T-T_H$  for each nonzero  $q_{ij}$ . Geometrically, the vicinity of this bifurcation point can be represented by two ellipsoidal 3D cones with touching tips in the 4D configuration space of  $T$ ,  $q_{11}$ ,  $q_{12}$ , and  $q_{22}$  [see Fig. 1(c) for a particular case of  $q_{12}=0$  when the cones are 2D surfaces]. Indeed, at a fixed value of  $|T-T_H|$  Eq. (28) defines an ellipsoid in the coordinates  $q_{ij}$ . In the full space of  $T$  and  $q_{ij}$ , there are two such ellipsoids lying in hyperplanes intersecting the temperature axis at  $\pm(T-T_H)$ . The dimensions of the ellipsoids scale linearly with  $|T-T_H|$  and shrink to a point at  $|T-T_H| \rightarrow 0$ , producing 3D double cone. If all components of  $q_{ij}$  are increased simultaneously in proportion to each other, then  $T-T_H$  increases, or, respectively, decreases, linearly with  $q_{ij}$ .

### 3. Isothermal path

A third example is an isothermal variation from the hydrostatic state  $H$ . Just as in the isobaric case, the system has three degrees of freedom. Equation (17) gives the phase equilibrium condition

$$-\Delta\bar{\Omega}(p-p_H) - \frac{1}{2} \left( \frac{\partial\Delta\Omega}{\partial p} \right)_H (p-p_H)^2 + \frac{\Omega_0^s}{2} \sum_{i,j=1,2} S_{ijkl} q_{ij} q_{kl} = 0. \quad (29)$$

If  $\Delta\bar{\Omega}$  is finite and the second term is small in a given pressure range, we obtain the equation

$$p - p_H = \frac{\Omega_0^s}{2\Delta\bar{\Omega}} \sum_{i,j,k,l=1,2} S_{ijkl} q_{ij} q_{kl}, \quad (30)$$

showing that the pressure change is quadratic in nonhydrostatic stresses. Combining Eqs. (3) and (30), the change in the chemical potential  $\mu^f$  in the fluid due to the deviation from the hydrostatic equilibrium along a path defined by solid-fluid coexistence at a constant  $T$  is

$$\mu^f(T_H, p) - \mu^f(T_H, p_H) = \frac{\bar{\Omega}^f \Omega_0^s}{2\Delta\bar{\Omega}} \sum_{i,j,k,l=1,2} S_{ijkl} q_{ij} q_{kl}. \quad (31)$$

Similarly to the isobaric variation, the change in chemical potential is quadratic in nonhydrostatic stresses. Crystallization of the fluid to a hydrostatic solid is accompanied by a change in the chemical potential

$$\mu^f(T_H, p) - \mu_*^s(T_H, p) = \Delta\bar{\Omega}(p - p_H) = \frac{\Omega_0^s}{2} \sum_{i,j=1,2} S_{ij} q_{ij}, \quad (32)$$

where we used the chemical potential of a hydrostatic solid

$$\mu_*^s(T_H, p) = \mu^f(T_H, p_H) + \bar{\Omega}^s(p - p_H). \quad (33)$$

Since the right-hand side of Eq. (32) is positive, the liquid is unstable against crystallization to a hydrostatic solid.

For a special point with  $\Delta\bar{\Omega}=0$ , the linear term in Eq. (29) drops out and we obtain

$$(p - p_H)^2 = \frac{\Omega_0^s}{\left(\frac{\partial\Delta\bar{\Omega}}{\partial p}\right)_H} \sum_{i,j,k,l=1,2} S_{ijkl} q_{ij} q_{kl}. \quad (34)$$

If  $(\partial\Delta\bar{\Omega}/\partial p)_H < 0$ , this equation has only a zero solution so that any nonhydrostatic stress applied at constant  $T$  destroys the phase equilibrium. If  $(\partial\Delta\bar{\Omega}/\partial p)_H > 0$ , the hydrostatic state is a bifurcation point generating two different equilibrium pressures  $\pm(p - p_H)$  for each set of nonhydrostatic stresses  $q_{ij}$ . The geometric model of touching cones is again valid but the configuration space is now  $p, q_{ij}$  [in Fig. 1(c), the  $T$  axis is replaced by  $p$ ]. Increasing all components of  $q_{ij}$  in proportion to each other results in a linear shift of the equilibrium pressure up or down.

### B. Deformation of a solid in equilibrium with the same fluid

So far we have only discussed equilibrium processes in which the solid-fluid system deviates away from its initial hydrostatic state along a hydrostatic, isobaric, or isothermal paths. We will now consider equilibrium processes in which both  $T$  and  $p$  remain constant. Because temperature and pressure uniquely define the state of a single-component fluid, it is only the solid that can change its state due to the additional degrees of freedom associated with the nonhydrostatic stresses  $q_{11}$ ,  $q_{12}$ , and  $q_{22}$ . Due to these degrees of freedom, solids in different nonhydrostatic states can be equilibrated with the same fluid. We will refer to such states as ‘‘isofluid’’ states. Accordingly, processes in which the solid changes its state while maintaining equilibrium with the same fluid will be called isofluid process.

The equation of isofluid processes is obtained from Eq. (17) by fixing the values of  $T - T_H$  and  $p - p_H$ . The general form of this equation is

$$\sum_{i,j=1,2} S_{ijkl} q_{ij} q_{kl} = \text{const}, \quad (35)$$

describing an ellipsoid in the 3D space of  $q_{11}$ ,  $q_{12}$ , and  $q_{22}$ . If the constant in this equation is zero, the ellipsoid shrinks to a point and the only solution is  $q_{ij}=0$ , which precludes any processes. If the constant is not zero, the ellipsoid has finite dimensions and does not contain a point at which  $q_{ij}=0$ . Thus, an isofluid path cannot contain a hydrostatic point. The solid must always remain in a nonhydrostatic state.

As a simple illustration, consider processes in which  $q_{12}$  remains zero. At a fixed pressure, the equilibrium temperature is a function of the principal nonhydrostatic stresses  $q_{11}$  and  $q_{22}$ . For a nonspecial point, this function is given by Eq. (24) and its plot is a paraboloid shown in Fig. 1(b). The plane  $T = \text{const}$  intersects the paraboloid along an ellipse on which both  $p$  and  $T$  are constant and thus the state of the fluid is fixed. This ellipse contains all isofluid processes possible in the system (at  $q_{12}=0$ ). During such processes, the solid undergoes a compression along one principal direction of stress and simultaneous tension along the other direction so that Eq. (35) is satisfied.

Referring to Fig. 1(b), one can imagine that if the temperature increases, the size of the ellipse decreases until it collapses to a single point at  $T \rightarrow T_H$ . At this point the isothermal plane touches the paraboloid at the hydrostatic point ( $T = T_H, q_{11} = q_{22} = 0$ ), prohibiting any changes in the state of the solid without changing the state of the fluid. This construction graphically illustrates the impossibility of isofluid processes passing through a hydrostatic state. The latter conclusion remains valid for special points, which is evident from examining the double-cone plot in Fig. 1(c).

Isofluid processes can also be represented by ellipsoidal surfaces (ellipses if  $e_{12} = \text{const}$ ) in terms of lateral strains instead of stresses. An expression for the slope  $(de_{22}/de_{11})_{T,p,e_{12}}$ , which will be used Part II of this work,<sup>5</sup> is derived in Appendix C.

## III. METHODOLOGY OF ATOMISTIC SIMULATIONS

In this section we describe our methodology of atomistic simulations of solid-liquid equilibrium. The simulations included nonhydrostatic variations of two types: (i) at zero pressure in the liquid (isobaric path) and (ii) at constant temperature (isothermal path). As the initial hydrostatic state  $H$  we chose the liquid at zero pressure and the stress-free solid in equilibrium with each other. For the material which we study, this state is not a special point, i.e., both  $\Delta\bar{\Omega}$  and  $\Delta\bar{s}$  are finite. Furthermore, within the range of simulated nonhydrostatic stresses,  $\Delta\bar{\Omega}$  and  $\Delta\bar{s}$  vary but do not go through zero.

### A. Simulated models

We used copper as a model material with interactions between atoms described with an embedded-atom potential.<sup>15</sup>

The potential was obtained by fitting to experimental and first-principles data and accurately reproduces the lattice parameter, cohesive energy, elastic constants, thermal expansion, and other relevant properties of copper. The melting point of Cu predicted by this potential is  $T_H=1327$  K in a good agreement with experiment (1356 K).<sup>16</sup>

The simulation block composed of 23 040 atoms contained a layer of solid phase sandwiched between two liquid layers. The (110)-oriented solid-liquid interfaces were perpendicular to the  $z$  direction of the block. The  $x$  and  $y$  directions were parallel to crystallographic directions  $[\bar{1}10]$  and  $[001]$ , respectively. The boundary conditions in the  $x$  and  $y$  directions were periodic. Two types of boundary conditions were used in the  $z$  direction. For simulations at constant zero pressure in the liquid, the liquid layers were terminated at open surfaces. The exposure of the liquid layers to vacuum ensured  $p=0$  in the liquid. For isothermal simulations, periodic boundary conditions were applied in the  $z$  direction.

To create nonhydrostatic states of stress in the solid, the block was subject to tensile or compressive deformations parallel to the coordinate axes by scaling the respective dimensions of the block. Due to crystallographic symmetry of the solid, the principal axes of stress and strain coincide and are parallel to the coordinate axes. For example, an applied biaxial strain creates a biaxial state of stress.

Four types of deformation were applied to the initially hydrostatic simulation block: (i) biaxial compression parallel to the lateral directions  $x$  and  $y$ , (ii) biaxial tension in the  $x$  and  $y$  directions, (iii) compression in  $x$  with simultaneous tension in  $y$ , and (iv) compression in  $y$  with simultaneous tension in  $x$ . All strains applied are listed in Tables II and III together with the stresses that arise. The stress components range from  $-2.3$  to  $3.4$  GPa. In some of the cases (iii) and (iv),  $\sigma_{11}$  and  $\sigma_{22}$  were close to each other in magnitude but opposite in sign so that the trace ( $\sigma_{11}+\sigma_{22}+\sigma_{33}$ ) was small.

Application of strain to the initially stress-free block destroyed the phase equilibrium. To re-equilibrate the phases at a constant zero pressure or at a constant temperature, different MD ensembles were implemented as explained below.

### B. Simulations at constant zero pressure in the liquid

To equilibrate the phases at  $p=0$  in the liquid, a 2-ns-long MD run in microcanonical ( $NVE$ ) ensemble was performed.<sup>17</sup> The zero pressure in the liquid was maintained by the liquid surfaces. During the equilibration, the temperature changed from the initial  $T_H$  to an equilibrium value  $T$  as a result of partial melting or crystallization of the phases. For example, if a part of the solid melts, the potential energy of the system increases by the amount of latent heat expended for the melting. To keep the total energy of the system constant, this heat is taken from the kinetic energy of atoms, resulting in a decrease in temperature. This temperature decrease reduces and eventually reverses the thermodynamic driving force of melting. Similar processes occur during partial crystallization of the liquid. As a result, after equilibration the temperature and the amounts of phases fluctuate around their equilibrium average values by spontaneous melting-crystallization processes. To verify that the system

has reached the true equilibrium, we checked that the temperature and energy distributions were Gaussian. We also verified that the average amounts of solid and liquid phases remained constant after the equilibration.

The equilibration stage was followed by a 40 ns production run using again  $NVE$  ensemble. During this run, snapshots of the system were saved every 0.01 ns. The snapshots contained information about positions and energies of all atoms, as well as the atomic stresses. These data were used at the postprocessing stage. The equilibrium temperatures  $T$  reported below were computed by averaging over the production stage.

### C. Simulations at constant temperature

Isothermal equilibration was achieved by a 2 ns MD run in the canonical ( $NVT$ ) ensemble using a Noose-Hoover thermostat at  $T_H$  and all periodic boundary conditions. During the run, the liquid pressure  $p$  changes from zero to an equilibrium value. The equilibration is reached due to the constant volume of the system and the existence of the volume effect of melting. Indeed, consider a fluctuation in which a small part of the solid melts or crystallizes. Because the atomic volume of solid Cu,  $\Omega^s$ , is smaller than the atomic volume of liquid Cu,  $\Omega^l$ , in the simulated temperature and strain range, this fluctuation results in an increase, or, respectively, decrease, of pressure in the liquid. This change in  $p$  counteracts further melting or crystallization and eventually stops them. As a result,  $p$  begins to fluctuate around an equilibrium value. As in the isobaric case, the equilibration was followed by a 40 ns  $NVT$  production run to compute the pressure and stress and to produce snapshots for subsequent postprocessing.

### D. Calculation of elastic constants and elastic compliances

To compare the MD results with the equilibrium temperatures and pressures predicted by Eqs. (24) and (30), we needed to know the elastic compliances of the material at  $T_H$ . The elastic constants and compliances were computed by MD simulations in the  $NVT$  ensemble at  $T_H$  using a Noose-Hoover thermostat. The solid block with periodic boundary conditions in all directions had the same crystallographic orientation and dimensions as the solid layer in the solid-liquid simulations. To compute the components of the elastic constant tensor  $C_{ijkl}$ , three different types of elastic deformations were applied to the initially unstressed solid. Each time the block was deformed along one of the principal axes of strain, keeping two other components of strain zero. During subsequent MD simulations at  $T_H$ , the stresses produced by the deformation were computed for each of the three directions of the strain. The elastic constants  $C_{ijkl}$  were computed from linear fits of stress versus strain. Inverting the elastic constants tensor gives the elastic compliances tensor  $S_{ijkl}$ .

## IV. RESULTS

### A. Phase coexistence surface

Due to crystal symmetry and the geometric setup of our system, the principal axes of the stress and strain coincide

TABLE I. Elastic constants and elastic compliances of Cu at  $T_H=1327$  K with  $[\bar{1}10]$ ,  $[001]$ , and  $[110]$  crystallographic directions aligned with  $x$ ,  $y$ , and  $z$  axes. Due to crystal symmetry, there are only four distinct elastic constants (compliances), only three of which are independent. The two-index elastic constants in the cubic system at  $T_H$  are  $c_{11}=106.6$  GPa,  $c_{12}=86.4$  GPa, and  $c_{44}=41.1$  GPa, which are smaller than the 0 K values  $c_{11}=169.9$  GPa,  $c_{12}=122.6$  GPa, and  $c_{44}=76.2$  GPa (Ref. 15).

Elastic constants	$C_{1111}$	$C_{2222}$	$C_{3333}$	$C_{1122}$	$C_{1133}$	$C_{2233}$
Value (GPa)	137.6	105.7	137.6	86.4	55.5	86.4
Elastic compliances	$S_{1111}$	$S_{2222}$	$S_{3333}$	$S_{1122}$	$S_{1133}$	$S_{2233}$
Value ( $10^4$ GPa $^{-1}$ )	157.7	353.8	157.7	-158.4	35.9	-158.4

with the coordinate axes, resulting in  $q_{12}=0$  in the stressed solid. At  $p=0$ , the heat of melting equals the difference,  $\Delta\bar{u}$ , between the energies per atom of the phases. Equation (24) thus reduces to

$$T - T_H = -\frac{\bar{\Omega}^s T_H}{2\Delta\bar{u}} [S_{1111}\sigma_{11}^2 + 2S_{1122}\sigma_{11}\sigma_{22} + S_{2222}\sigma_{22}^2]. \quad (36)$$

For isothermal variations at  $T=T_H$  and  $q_{12}=0$ , Eq. (30) becomes

$$p - p_H = \frac{\bar{\Omega}^s T_H}{2\Delta\bar{\Omega}} [S_{1111}q_{11}^2 + 2S_{1122}q_{11}q_{22} + S_{2222}q_{22}^2]. \quad (37)$$

Table I summarizes the elastic constants and elastic compliances of the solid computed by MD simulations at  $T_H$  for the particular crystallographic orientation implemented in this work. The elastic constants recomputed to the cubic coordinate system and expressed via the standard two-index notations  $c_{ij}$  are included in the caption to Table I. For the hydrostatic state at temperature  $T_H$ , the energies per atom in the solid and liquid phases were found to be  $\bar{u}^s = -3.17$  eV and

$\bar{u}^l = -3.04$  eV, respectively, giving the latent heat  $\Delta\bar{u} = 0.13$  eV. The atomic volumes of the phases at  $T_H$  were  $\bar{\Omega}^s = 12.75$  Å $^3$  and  $\bar{\Omega}^l = 13.37$  Å $^3$ , respectively. Using these data, we computed the equilibrium temperatures  $T$  at zero pressure in the liquid from Eq. (36) and the equilibrium liquid pressures  $p$  at constant temperature  $T_H$  from Eq. (37) for a set of nonhydrostatic stresses  $q_{ij}$ . The results are reported in Figs. 2–4 and in Tables II and III.

We will now compare these theoretical predictions with results of MD simulations. For isobaric variations, Table II demonstrates that, for biaxial stresses, the predicted temperatures agree with the MD results within 1 K or better, except for the largest stress when the discrepancy reaches 4.6 K. For some of the mixed tension-compression loads associated with relatively large strains, the discrepancies become larger. Nevertheless, the entire set of MD points shows a very close agreement with the paraboloidal coexistence surface predicted by Eq. (36) (Fig. 2). In particular, for all stresses tested, the coexistence temperature is reduced in comparison with  $T_H$  independently of the signs of the stress components. Furthermore, calculations from Eq. (36) demonstrate excellent agreement with MD simulations for the biaxial tension and compression paths as shown in Fig. 3.

In addition, the MD results directly confirm that the hydrostatic part of the stress tensor,  $\bar{p} = -(\sigma_{11} + \sigma_{22} + \sigma_{33})/3$ , is not a meaningful physical parameter to characterize the effect of stresses on phase equilibrium. As was discussed by Sekerka and Cahn,<sup>4</sup> previous theories attempting to fold the

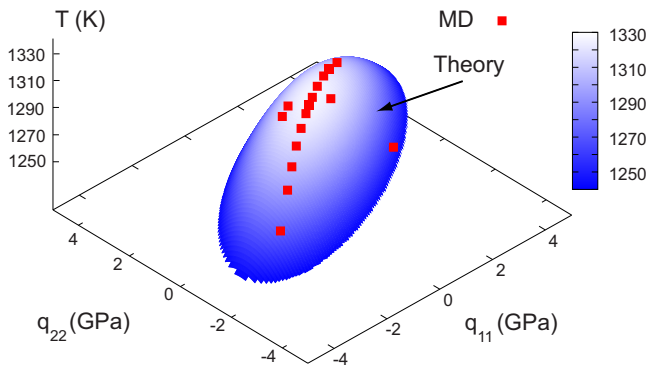


FIG. 2. (Color online) Equilibrium temperature  $T$  as a function of lateral stresses  $\sigma_{11}$  ( $[\bar{1}10]$  direction) and  $\sigma_{22}$  ( $[001]$  direction) in the solid computed for copper with the  $(110)$  solid-liquid interface. Pressure in the liquid remains zero. The solid (blue) surface is the theoretical prediction from Eq. (36), the red points are results of direct MD simulations.

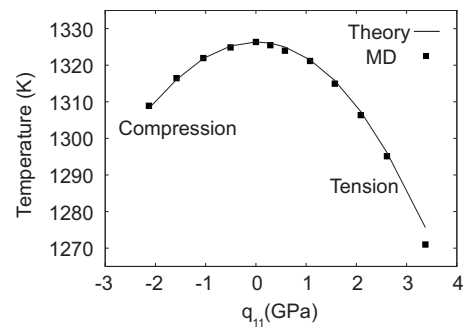


FIG. 3. Equilibrium temperature as a function of the nonhydrostatic stress component  $q_{11}$  in the solid subject to biaxial tension or compression. Pressure in the liquid remains zero. The points are results of direct MD simulations, the line was computed from Eq. (36).

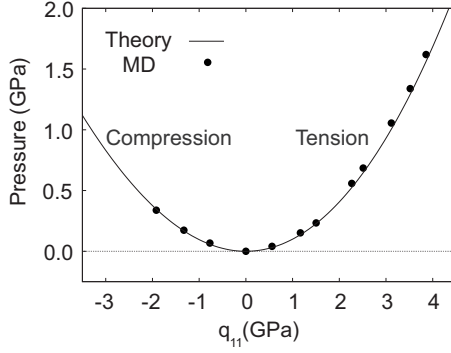


FIG. 4. Equilibrium pressure in the liquid as a function of the nonhydrostatic stress component  $q_{11}$  in the solid subject to biaxial tension or compression at a constant temperature  $T_H$ . The points are results of direct MD simulations, the line was computed from Eq. (37).

stress effect into the “solid pressure”  $\bar{p}$  were erroneous. For example, the last but one line in Table II refers to a mixed-load case when  $\sigma_{11}=0.448$  GPa,  $\sigma_{22}=-0.489$  GPa, and  $\sigma_{33}=0$ , thus giving a very small solid pressure  $\bar{p}=-0.014$  GPa. Nonetheless, the reduction in temperature of about 10 K found for this case is close to that for biaxial compression by  $e_{11}=-0.895\%$  when  $\bar{p}=0.833$  GPa and for biaxial tension by  $e_{11}=0.928\%$  when  $\bar{p}=-0.864$  GPa. This example is a clear demonstration that it is the combination of nonhydrostatic stress components  $q_{ij}$  appearing in the right-hand side of Eq. (36) that determines the temperature depression  $T-T_H$ , not  $\bar{p}$  alone.

For isothermal variations at  $T=T_H$  (Table III), the equilibrium liquid pressure increases as the solid deviates from the hydrostatic state of stress regardless of the sign of the devia-

tion. Figure 4 shows an excellent agreement between the liquid pressures predicted theoretically from Eq. (37) and obtained by MD simulations for biaxial tension and compression.

### B. Instability of nonhydrostatic systems

As discussed in Sec. II, a liquid equilibrated with a nonhydrostatically stressed solid is unstable or metastable and should eventually crystallize into a hydrostatically stressed solid. The liquid is metastable when there is a nucleation barrier that prevents it from immediate crystallization into a hydrostatic solid. If liquid is equilibrated with a solid under sufficiently large nonhydrostatic stresses, the barrier can be reduced to a level when crystallization can be observed on a given time scale.

To verify this prediction, we performed MD simulations of a solid-liquid system in which the solid was stressed by  $\sigma_{11}=2.3$  GPa and  $\sigma_{22}=3.4$  GPa. As above, the *NVE* ensemble was implemented to bring the system to phase equilibrium at  $p=0$ , which was reached at  $T=1271$  K (66 K below  $T_H$ ). The size of the simulation block was then increased to 207 360 atoms by multiplying the  $x$  and  $y$  dimensions by a factor of three while keeping the same dimension in the  $z$  direction. The ensemble was switched to *NVT* to allow heat absorption by a thermostat should crystallization begin.

After 0.12 ns of the *NVT* simulation, the liquid began to crystallize. Figure 5(a) shows a typical snapshot of the simulation block during the crystallization process. The block contains a region of the initial solid under tension, newly crystallized solid regions, and the remaining liquid. The stress profiles [Fig. 5(b)] reveal that the initial solid has ap-

TABLE II. Lateral strains and stresses in the solid and the corresponding solid-liquid equilibrium temperatures predicted by Eq. (36) ( $T_{Theor}$ ) and computed directly from MD simulations ( $T_{MD}$ ) for variations at constant zero pressure in the liquid.

$e_{11}$ (%)	$e_{22}$ (%)	$\sigma_{11}$ (GPa)	$\sigma_{22}$ (GPa)	$T_{MD}$ (K)	$T_{Theor}$ (K)
-1.196	Biaxial	-2.147	-1.262	1308.9	1308.2
-0.895	Biaxial	-1.563	-0.936	1316.5	1316.1
-0.593	Biaxial	-1.048	-0.642	1321.9	1321.8
-0.290	Biaxial	-0.509	-0.322	1324.9	1325.2
0.000	Biaxial	0.004	-0.009	1326.4	1326.4
0.165	Biaxial	0.286	0.167	1325.5	1326.0
0.333	Biaxial	0.577	0.350	1324.0	1325.0
0.628	Biaxial	1.077	0.674	1321.2	1321.5
0.928	Biaxial	1.583	1.010	1315.0	1315.8
1.236	Biaxial	2.095	1.360	1306.4	1307.3
1.544	Biaxial	2.604	1.714	1295.0	1296.1
2.020	Biaxial	3.394	2.282	1271.0	1275.6
-3.399	5.559	-1.652	1.480	1267.7	1242.3
2.240	-3.469	0.720	-0.433	1309.6	1315.9
1.798	-2.899	0.448	-0.489	1315.2	1318.5
-0.960	1.4709	-0.414	0.301	1323.0	1322.2

TABLE III. Biaxial lateral strains, stresses in the solid, and the equilibrium pressures in the liquid predicted by Eq. (37) ( $p_{Theor}$ ) and computed directly from MD simulations ( $p_{MD}$ ) for isothermal variation at  $T_H$ .

$e$ (%)	$\sigma_{11}^s$ (GPa)	$\sigma_{22}^s$ (GPa)	$p_{MD}$ (GPa)	$p_{Theor}$ (GPa)
-1.155	-2.256	-1.479	0.339	0.348
-0.803	-1.501	-0.970	0.174	0.168
-0.466	-0.838	-0.552	0.068	0.059
0.000	0.000	0.000	0.000	0.000
0.300	0.519	0.296	0.041	0.030
0.631	1.015	0.590	0.152	0.135
0.803	1.269	0.723	0.234	0.225
1.155	1.709	0.920	0.558	0.523
1.266	1.827	0.965	0.686	0.647
1.503	2.058	1.014	1.056	1.005
1.650	2.180	1.015	1.339	1.292
1.740	2.238	0.979	1.619	1.563

proximately the same stresses as prior to the crystallization. The new solid regions grow under a much smaller stress and are nearly hydrostatic (within uncertainties caused by fluctuations). The stress in the liquid layers is equally small and also nearly hydrostatic as it should. The peaks at the liquid surfaces are due to the surface tension. During the subsequent 0.5 ns time the remaining liquid crystallizes completely.

Upon completion of crystallization, the block contains two solid-solid interfaces separating layers of the same material with the same crystallographic orientation but slightly different lattice constants due to different stress states. The lattice misfit between the old and new solid regions is accommodated by  $\frac{1}{2}[110]$  edge dislocations,<sup>18,19</sup> which were identified by construction of Burger circuits. These dislocations dissociate into Shockley partials on  $\{111\}$  gliding planes, which are not parallel to the interfaces. As a result,

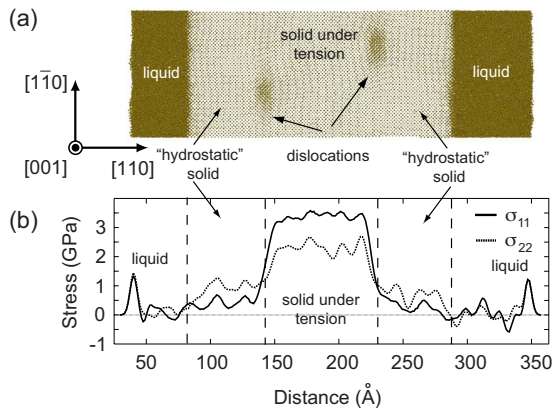


FIG. 5. (Color online) (a) Snapshot of the simulation block during crystallization at  $T=1271$  K. (b) Profiles of the lateral components of stress  $\sigma_{11}$  and  $\sigma_{22}$  across the simulation block. Before the crystallization, the stresses in the solid were  $\sigma_{11}=3.4$  GPa and  $\sigma_{22}=2.3$  GPa.

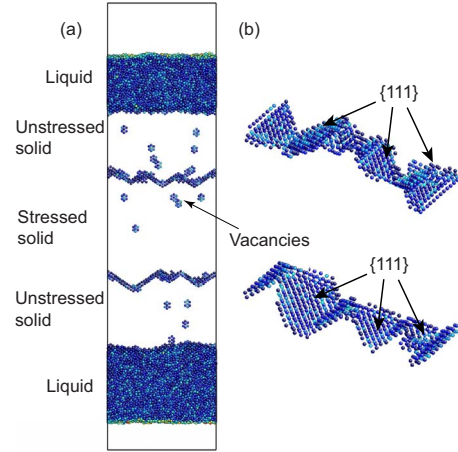


FIG. 6. (Color online) (a) Simulation block with edge dislocations visualized using central symmetry analysis. Atoms with large values of the symmetry parameter are invisible (Ref. 20). (b) Different views of  $\frac{1}{2}[110]$  edge dislocations showing its dissociation into partials.

the dislocation lines are not straight but have zigzag shapes with  $\langle 211 \rangle$  segments dissociated on  $\{111\}$  facets. Figure 6(a) shows the entire simulation block with the solid-solid interfaces while Fig. 6(b) illustrates separately the zigzag dislocation lines with dissociated segments. The solid contains a few vacancies revealed by the centrosymmetry parameter.

The delayed start of the crystallization is consistent with the existence of a nucleation barrier. Furthermore, similar simulations in a block containing only 23 040 atoms did not produce a crystallization on time scales accessible by MD, suggesting that the barrier is size dependent.

## V. DISCUSSION AND CONCLUSIONS

As pointed out in Sec. I, the problem of solid-fluid equilibrium discussed in this paper is relevant to many materials phenomena and applications. It is important to have a clear understanding of the effect of nonhydrostatic stresses on solid-fluid equilibrium. Unfortunately, literature contains a number of misconceptions, such as the solid pressure discussed in Sec. IV A.

For a single-component system, Gibbs<sup>2</sup> derived an equation (406) which is similar to our Eq. (5) and to Sekerka and Cahn's<sup>4</sup> Eq. (14) (they assumed  $dp=0$ ). On p. 199 Gibbs pointed out that if  $p=\text{const}$ , equation (406) can be used for predicting how the equilibrium temperature is affected by strain variations in the solid. He then noted that if the initial state of the solid is hydrostatic, the differentials of temperature with respect to strain components vanish. This comment can be understood, although it was not stated by Gibbs explicitly, that nonhydrostatic deformations produce high-order effects on equilibrium temperature.

Sekerka and Cahn<sup>4</sup> employed isotropic linear elasticity to show that this effect is quadratic in nonhydrostatic stresses  $q_{ij}$ , which is consistent with Gibbs. Their analysis was focused on isobaric variations from a hydrostatic state and assumed a nonzero latent heat (a nonspecial point).

In this paper we have extended Sekerka and Cahn's work<sup>4</sup> in several ways. We treat elastic deformations of the solid using anisotropic linear elasticity and a generalized Hooke's law which includes the thermal-expansion effect  $\eta$ , see Eq. (6). In the future, this approach could be readily generalized to multicomponent systems, in which  $\eta$  is a function of not only temperature but also chemical composition (compositional strain).<sup>21</sup> Our main result is expressed by Eq. (17) which relates deviations of the equilibrium temperature, pressure, and lateral stress components from their hydrostatic values. This equation permits predictions of the nonhydrostaticity effect on the equilibrium temperature and pressure. Furthermore, this effect has been analyzed not only for nonspecial points considered by Gibbs<sup>2</sup> and Sekerka and Cahn<sup>4</sup> but also special points where the latent heat or volume effect go through zero. To make our equations and their ramifications more intuitive, we have presented a geometric interpretation of the phase coexistence surface as a quadric or its sections by appropriate planes.

For nonspecial points, our analysis predicts that if pressure in the liquid is fixed, the change in the equilibrium temperature is quadratic in  $q_{ij}$ , which is in agreement with Sekerka and Cahn's result for isotropic solids.<sup>4</sup> If temperature is fixed, the change in the equilibrium pressure is quadratic in  $q_{ij}$ . If both temperature and pressure are fixed, which fixes the thermodynamic state of the fluid, the stress state of the solid can still be varied along a so-called isofluid path without violating the phase coexistence. In short, the same fluid can be equilibrated with many solids, all of which are nonhydrostatic.

In special points, the stress effect can be very different from that in nonspecial points. Depending on the material properties, nonhydrostatic stresses can either completely destroy the phase coexistence or produce a bifurcation in which the equilibrium temperature or pressure can either increase or decrease. Special points exist in a number of systems. It would be interesting to test our predictions for such systems by experiment or atomistic simulations in the future.

Our analysis for nonspecial points has been tested against MD simulations of solid-liquid equilibrium in copper. Very encouraging agreement has been observed between our theory and the simulations for both isobaric and isothermal variations from hydrostatic equilibrium.

Another interesting effect studied in this work is the instability of the fluid with respect to crystallization to a hydrostatic solid. This instability was discussed in detail by Gibbs<sup>2</sup> (p. 196–197) who showed that the chemical potential of the solid component in a fluid equilibrated with a nonhydrostatic solid is greater than in a fluid equilibrated with a hydrostatic solid at the same temperature and pressure. Gibbs concluded that the fluid is always supersaturated with respect to the solid component unless the solid is hydrostatic. He predicted that, if a fluid equilibrated with a nonhydrostatic solid contains a fragment of hydrostatic solid composed of the same substance, this fragment will tend to grow. Even if such fragments are not present in the fluid, Gibbs asserted that layers of hydrostatically stressed solid will grow on the surface of the nonhydrostatically distorted solid.

Formally, this latter prediction has been verified by our MD simulations, in which a nearly stress-free solid layer was

found to grow on top of a stressed solid (Figs. 5 and 6). It should be noted, however, that Gibbs' discussion was for a fluid that contained not only the component of the solid (Gibbs always assumed that a homogeneous solid could be composed of only one component) but also at least one other component insoluble in the solid.<sup>22</sup> It is only under this condition that the chemical potential of the solid component in the fluid could vary at a fixed temperature and pressure.

By contrast, our analysis as well as simulations were for a truly single-component system. Nevertheless, we have shown that the chemical potential of a single-component fluid equilibrated with a nonhydrostatic solid composed of the same component is always larger than the chemical potential of a hydrostatic solid at the same temperature and pressure. Specifically, the chemical-potential differences for isobaric and isothermal deformations are given by Eqs. (27) and (32), respectively. This result is especially intuitive when  $\Delta\bar{h} > 0$ , as in our simulations for the melting of copper. In this case Eq. (24) predicts that the fluid equilibrated with a nonhydrostatic solid is overcooled relative to the hydrostatic melting point. This overcooled fluid is ready to crystallize to a hydrostatic solid. It is important to recognize that Eqs. (27) and (32) are valid regardless of the signs of the latent heat or the transformation volume. In particular, since the latent heat of melting of <sup>3</sup>He is negative at temperatures below the minimum of the melting pressure,<sup>9,10</sup> the liquid equilibrated with a nonhydrostatic solid is overheated relative to the hydrostatic state. Nevertheless, this liquid is still unstable against crystallization to a hydrostatic solid. This fact, which was noted by Sekerka and Cahn (their footnote 7),<sup>4</sup> follows immediately from Eq. (27). Likewise, nonhydrostatic distortions destabilize not only typical materials with  $\Delta\bar{\Omega} > 0$  but also Si, Ge, and other elements whose density increases upon melting.

Thus, our analysis shows that the Gibbsian prediction of crystallization of hydrostatic layers on surfaces of nonhydrostatically distorted solids remains valid also for single-component systems. Although we arrived at this conclusion in Sec. II assuming linear elasticity and the small-strain approximation, it actually reflects a general rule. In Appendix D we derive this rule from general principles of thermodynamics without any approximations.

Finally, some of our results can be applied to incoherent solid-solid interfaces. If the system is deformed along a path on which one of the phases remains hydrostatic while the other is not, our equations can be applied by formally treating the hydrostatic phase as a "fluid."

## ACKNOWLEDGMENTS

This work was supported by the U.S. Department of Energy, Office of Basic Energy Sciences. We acknowledge useful discussions facilitated through coordination meetings sponsored by the DOE-BES Computational Materials Science Network (CMSN) program.

## APPENDIX A: MAXWELL RELATIONS FOR AN ELASTIC SOLID

In this appendix we derive Maxwell relations for a single-component solid phase whose elastic properties are described

by Eq. (6) with a constant compliance tensor  $S_{ijkl}$ . Consider a thermodynamic function  $\phi$  per atom of the solid phase, defined by

$$\phi = u^s - Ts^s + p\Omega^s. \quad (\text{A1})$$

Here,  $-p$  is the principal component  $\sigma_{33}$  of the stress tensor whose other principal components are not necessarily equal to  $-p$ . Differentiating  $\phi$  and using Eqs. (2) and (4), we obtain

$$d\phi = -s^s dT + \Omega^s dp + \Omega_0^s \sum_{i,j=1,2} q_{ij} de_{ij}. \quad (\text{A2})$$

After substituting  $e_{ij}$  from Eq. (6), this equation becomes

$$d\phi = -\left(s^s - \Omega_0^s \sum_{i,j=1,2} q_{ij} \eta'_{ij}\right) dT + \left(\Omega^s - \Omega_0^s \sum_{i,j,m=1,2,3} q_{ij} S_{ijmm}\right) dp + \Omega_0^s \sum_{i,j,k,l=1,2} S_{ijkl} q_{ij} dq_{kl}. \quad (\text{A3})$$

Since Eq. (A3) is a perfect differential in the variables  $T$ ,  $p$ ,  $q_{11}$ ,  $q_{12}$ , and  $q_{22}$ , the following Maxwell relations must be satisfied

$$-\frac{\partial\left(s^s - \Omega_0^s \sum_{i,j=1,2} q_{ij} \eta'_{ij}\right)}{\partial q_{kl}} = \frac{\partial\left(\Omega_0^s \sum_{i,j=1,2} S_{ijkl} q_{ij}\right)}{\partial T}, \quad k, l = 1, 2, \quad (\text{A4})$$

$$\frac{\partial\left(\Omega^s - \Omega_0^s \sum_{i,j,m=1,2,3} q_{ij} S_{ijmm}\right)}{\partial q_{kl}} = \frac{\partial\left(\Omega_0^s \sum_{i,j=1,2} S_{ijkl} q_{ij}\right)}{\partial p}, \quad k, l = 1, 2, \quad (\text{A5})$$

$$-\frac{\partial\left(s^s - \Omega_0^s \sum_{i,j=1,2} q_{ij} \eta'_{ij}\right)}{\partial p} = \frac{\partial\left(\Omega^s - \Omega_0^s \sum_{i,j,m=1,2,3} S_{ijmm} q_{ij}\right)}{\partial T}. \quad (\text{A6})$$

In Eqs. (A4) and (A5), the terms in the right-hand side are independent of  $T$  and  $p$  and the partial derivatives are zero. In Eq. (A6), the derivatives are computed at fixed  $q_{ij}$ . Thus, the terms containing  $q_{ij}$  vanish. The final form of these relations is given by Eqs. (8)–(10) in the main text.

## APPENDIX B: NONHYDROSTATIC STRESS-STRAIN TRANSFORMATION

We will derive an expression for the temperature change at a constant pressure  $p$  in terms of strains instead of nonhydrostatic stresses. For convenience of the derivation, we will use the matrix form of Hooke's law obtained by inversion of Eq. (6)

$$\hat{\sigma} = \mathbf{C} \cdot (\hat{e} - \hat{\eta}). \quad (\text{B1})$$

Here  $\hat{\sigma}$  and  $\hat{e}$  are columns containing six different components of the stress and strain tensors, respectively,  $\mathbf{C}$  is a  $6 \times 6$  symmetrical matrix of elastic constants, and the dot denotes matrix-column multiplication (contraction). The thermal strain is also represented by a column  $\hat{\eta}$  whose six components depend on  $T - T_0$ . The order in which we list the components of the stress and strain tensors is dictated by the goal of our calculation and is different from the standard Voigt notation. Specifically, we first list the lateral components of the stress and strain followed by the components related to the solid-fluid interface:

$$\hat{\sigma} = \begin{bmatrix} \sigma_{11} \\ \sigma_{22} \\ \sigma_{12} \\ \sigma_{13} \\ \sigma_{23} \\ \sigma_{33} \end{bmatrix} \equiv \begin{bmatrix} \sigma_1 \\ \sigma_2 \\ \sigma_3 \\ \sigma_4 \\ \sigma_5 \\ \sigma_6 \end{bmatrix}, \quad \hat{e} = \begin{bmatrix} e_{11} \\ e_{22} \\ 2e_{12} \\ 2e_{13} \\ 2e_{23} \\ e_{33} \end{bmatrix} \equiv \begin{bmatrix} e_1 \\ e_2 \\ e_3 \\ e_4 \\ e_5 \\ e_6 \end{bmatrix}, \quad \hat{\eta} = \begin{bmatrix} \eta_{11} \\ \eta_{22} \\ 2\eta_{12} \\ 2\eta_{13} \\ 2\eta_{23} \\ \eta_{33} \end{bmatrix} \equiv \begin{bmatrix} \eta_1 \\ \eta_2 \\ \eta_3 \\ \eta_4 \\ \eta_5 \\ \eta_6 \end{bmatrix}. \quad (\text{B2})$$

The matrix of the elastic constants is

$$\mathbf{C} = \begin{pmatrix} C_{1111} & C_{1122} & C_{1112} & C_{1113} & C_{1123} & C_{1133} \\ C_{2211} & C_{2222} & C_{2212} & C_{2213} & C_{2223} & C_{2233} \\ C_{1211} & C_{1222} & C_{1212} & C_{1213} & C_{1223} & C_{1233} \\ C_{1311} & C_{1322} & C_{1312} & C_{1313} & C_{1323} & C_{1333} \\ C_{2311} & C_{2322} & C_{2312} & C_{2313} & C_{2323} & C_{2333} \\ C_{3311} & C_{3322} & C_{3312} & C_{3313} & C_{3323} & C_{3333} \end{pmatrix} \equiv \begin{pmatrix} C_{11} & C_{12} & C_{13} & C_{14} & C_{15} & C_{16} \\ C_{21} & C_{22} & C_{23} & C_{24} & C_{25} & C_{26} \\ C_{31} & C_{32} & C_{33} & C_{34} & C_{35} & C_{36} \\ C_{41} & C_{42} & C_{43} & C_{44} & C_{45} & C_{46} \\ C_{51} & C_{52} & C_{53} & C_{54} & C_{55} & C_{56} \\ C_{61} & C_{62} & C_{63} & C_{64} & C_{65} & C_{66} \end{pmatrix}. \quad (\text{B3})$$

When the solid is hydrostatic at a temperature  $T_H$ , the stress components  $\sigma_1$ ,  $\sigma_2$ , and  $\sigma_6$  are identical and equal to  $-p$  whereas the three shear components are zero. This hydrostatic stress  $\hat{\sigma}_H$  and the respective strain  $\hat{e}_H$  satisfy Hooke's law

$$\hat{\sigma}_H = \mathbf{C} \cdot (\hat{e}_H - \hat{\eta}_H). \quad (\text{B4})$$

Here  $\hat{e}_H$  has the meaning of strain required for bringing the solid from the stress-free reference state at a temperature  $T_0$  to the hydrostatic state at temperature  $T_H$ .  $\hat{\eta}_H$  is the stress-free thermal strain measured when the temperature changes from  $T_0$  to  $T_H$ .

We choose the coordinate system so that the principal component of stress  $\sigma_6 = -p$  and the shear components  $\sigma_4$  and  $\sigma_5$  are zero. Furthermore, we choose  $T_H$  as the reference temperature  $T_0$ , resulting in  $\hat{\eta}_H = 0$ . Subtracting Eqs. (B1) and (B4) we obtain

$$\begin{bmatrix} q_1 \\ q_2 \\ q_3 \\ 0 \\ 0 \\ 0 \end{bmatrix} = \begin{pmatrix} C_{11} & C_{12} & C_{13} & C_{14} & C_{15} & C_{16} \\ C_{21} & C_{22} & C_{23} & C_{24} & C_{25} & C_{26} \\ C_{31} & C_{32} & C_{33} & C_{34} & C_{35} & C_{36} \\ C_{41} & C_{42} & C_{43} & C_{44} & C_{45} & C_{46} \\ C_{51} & C_{52} & C_{53} & C_{54} & C_{55} & C_{56} \\ C_{61} & C_{62} & C_{63} & C_{64} & C_{65} & C_{66} \end{pmatrix} \cdot \begin{bmatrix} E_1 - \eta_1 \\ E_2 - \eta_2 \\ E_3 - \eta_3 \\ E_4 - \eta_4 \\ E_5 - \eta_5 \\ E_6 - \eta_6 \end{bmatrix}, \quad (\text{B5})$$

where  $\hat{q} \equiv \hat{\sigma} - \hat{\sigma}_H$  and  $\hat{E} \equiv \hat{e} - \hat{e}_H$  are the nonhydrostatic stress and strain, respectively. The meaning of  $\hat{E}$  is the strain of bringing the solid from the hydrostatic state at temperature  $T_H$  to a given nonhydrostatic state at a temperature  $T$  and a constant pressure  $p$  in the fluid. The nonzero components  $q_1$ ,  $q_2$ , and  $q_3$  are the lateral components of the nonhydrostatic stress. All components of  $\hat{\eta}$  are functions of  $T - T_H$ .

Our next goal is to express the lateral components of  $\hat{q}$  in terms of the lateral components of  $\hat{E}$ . To this end, we rewrite Eq. (B5) in the form

$$\begin{bmatrix} \hat{q}_L \\ \hat{q}_\perp \end{bmatrix} = \begin{pmatrix} \mathbf{C}_1 & \mathbf{C}_2 \\ \mathbf{C}_3 & \mathbf{C}_4 \end{pmatrix} \cdot \begin{bmatrix} \hat{E}_L - \hat{\eta}_L \\ \hat{E}_\perp - \hat{\eta}_\perp \end{bmatrix}, \quad (\text{B6})$$

where we break  $\mathbf{C}$  into  $3 \times 3$  matrices  $\mathbf{C}_1$ ,  $\mathbf{C}_2$ ,  $\mathbf{C}_3$ , and  $\mathbf{C}_4$  and introduce the notations

$$\hat{q}_L \equiv \begin{bmatrix} q_1 \\ q_2 \\ q_3 \end{bmatrix}, \quad \hat{q}_\perp \equiv \begin{bmatrix} 0 \\ 0 \\ 0 \end{bmatrix}, \quad \hat{E}_L - \hat{\eta}_L \equiv \begin{bmatrix} E_1 - \eta_1 \\ E_2 - \eta_2 \\ E_3 - \eta_3 \end{bmatrix},$$

$$\hat{E}_\perp - \hat{\eta}_\perp \equiv \begin{bmatrix} E_4 - \eta_4 \\ E_5 - \eta_5 \\ E_6 - \eta_6 \end{bmatrix}. \quad (\text{B7})$$

Due to the symmetry of matrix  $\mathbf{C}$  [Eq. (B3)], matrices  $\mathbf{C}_1$  and  $\mathbf{C}_4$  are also symmetric while  $\mathbf{C}_2$  and  $\mathbf{C}_3$  are transpose of each other and generally not symmetric.

Equation (B6) can be rewritten as a system of two matrix equations

$$\hat{q}_L = \mathbf{C}_1 \cdot (\hat{E}_L - \hat{\eta}_L) + \mathbf{C}_2 \cdot (\hat{E}_\perp - \hat{\eta}_\perp), \quad (\text{B8})$$

$$0 = \mathbf{C}_2^T \cdot (\hat{E}_L - \hat{\eta}_L) + \mathbf{C}_4 \cdot (\hat{E}_\perp - \hat{\eta}_\perp), \quad (\text{B9})$$

where superscript  $T$  denotes transposition. Solving Eq. (B9) for  $\hat{E}_\perp - \hat{\eta}_\perp$  and inserting this in Eq. (B8), we arrive at the following expression for  $\hat{q}_L$  in terms of  $\hat{E}_L - \hat{\eta}_L$ :

$$\hat{q}_L = \mathbf{A} \cdot (\hat{E}_L - \hat{\eta}_L). \quad (\text{B10})$$

Here

$$\mathbf{A} \equiv \mathbf{C}_1 - \mathbf{C}_2 \cdot \mathbf{C}_4^{-1} \cdot \mathbf{C}_2^T \quad (\text{B11})$$

is a symmetric  $3 \times 3$  matrix. Equation (B10) can be inverted to

$$\hat{E}_L - \hat{\eta}_L = \mathbf{A}^{-1} \cdot \hat{q}_L. \quad (\text{B12})$$

Furthermore, it can be easily shown that

$$\mathbf{A}^{-1} = \mathbf{S}_L, \quad (\text{B13})$$

where  $\mathbf{S}_L$  is the upper-left-corner  $3 \times 3$  matrix of the  $6 \times 6$  matrix of compliances  $\mathbf{S}$  defined in a matter similar to Eq. (B5). Matrix  $\mathbf{S}$  appears in Hooke's law rewritten in our notations as  $\hat{E} - \hat{\eta} = \mathbf{S} \cdot \hat{q}$ . Using Eqs. (B10)–(B13), the quadratic form of  $q$ 's which frequently appears in our equations can now be written as

$$\sum_{i,j=1,2} S_{ijkl} q_{ij} q_{kl} = \hat{q}_L^T \cdot \mathbf{S}_L \cdot \hat{q}_L = q_L^T \cdot (\hat{E}_L - \hat{\eta}_L)$$

$$= (\hat{E}_L - \hat{\eta}_L)^T \cdot \mathbf{A} \cdot (\hat{E}_L - \hat{\eta}_L). \quad (\text{B14})$$

We can now derive an expression for the equilibrium temperature at a constant pressure. Changing variables in Eq. (23) by means of Eq. (B14) we obtain

$$\Delta \bar{s}(T - T_H) + \frac{1}{2} \left( \frac{\partial \Delta s}{\partial T} \right)_H (T - T_H)^2$$

$$+ \frac{\Omega_0^s}{2} \sum_{i,j=1,2,3} A_{ij} (E_i E_j - 2E_i \eta_j + \eta_i \eta_j) = 0. \quad (\text{B15})$$

If the hydrostatic state  $H$  is far enough from special points, Eq. (B15) reduces to

$$T - T_H = - \frac{\Omega_0^s T_H}{2 \Delta \bar{h}} \sum_{i,j=1,2,3} A_{ij} E_i E_j. \quad (\text{B16})$$

Combining Eqs. (3) and (B16), the respective change in the chemical potential in the fluid is

$$\mu^f(T, p_H) - \mu^f(T_H, p_H) = \frac{s^f \Omega_0^s T_H}{2 \Delta \bar{h}} \sum_{i,j=1,2,3} A_{ij} E_i E_j. \quad (\text{B17})$$

Thus, for isobaric variations from the hydrostatic state the changes in  $T$  and  $\mu^f$  are quadratic in lateral components of the strain.

### APPENDIX C: ISOFLUID EQUATIONS IN TERMS OF STRAINS

Equation (B15) can be applied to isofluid processes. Indeed, for a fixed temperature this equation defines an ellipsoid in the variables  $E_1$ ,  $E_2$ , and  $E_3$

$$\sum_{i,j=1,2,3} A_{ij}(E_i E_j - 2E_i \eta_j + \eta_i \eta_j) = \text{const.} \quad (\text{C1})$$

This ellipsoid is centered at point  $\hat{\eta}_L$  and represents the phase coexistence surface when the state of strain of the solid varies continuously at constant temperature and pressure, i.e., for a fixed state of the fluid.

Consider a particular isofluid path on which the shear strain  $E_3$  remains zero. In this case Eq. (C1) defines an ellipse (a cross section of the ellipsoid by the  $E_3=0$  plane) in the variables  $E_1$  and  $E_2$ . When the system undergoes a variation along this ellipse, the solid strained by an amount  $dE_1$  has to simultaneously contract by an amount  $dE_2$  to maintain the equilibrium with the fluid. To evaluate the derivative  $(dE_2/dE_1)_{T,p,E_3}$  along this path, we take a derivative of Eq. (C1) and take into account that at fixed  $T$  and  $p$  we have  $d\hat{E}=d\hat{e}$  and  $d\hat{\eta}_L=0$ . This gives

$$\left(\frac{dE_2}{dE_1}\right)_{T,p,E_3} = \left(\frac{de_{22}}{de_{11}}\right)_{T,p,e_{12}} = -\frac{A_{11}(E_1 - \eta_1) + A_{12}(E_2 - \eta_2)}{A_{21}(E_1 - \eta_1) + A_{22}(E_2 - \eta_2)}. \quad (\text{C2})$$

For cubic crystals thermal expansion is isotropic and  $\eta_1 = \eta_2$ . In particular, for a biaxially deformed cubic solid  $E_1 = E_2$  and Eq. (C2) becomes

$$\left(\frac{de_{22}}{de_{11}}\right)_{T,p,e_{12}} = -\frac{A_{11} + A_{12}}{A_{22} + A_{12}}. \quad (\text{C3})$$

Since our calculations assume that elastic properties are temperature independent, so is the right-hand side of this equation.

Calculations of matrix  $\mathbf{A}$  are simplified in the presence of crystal symmetry. For example, if the solid-fluid interface has the point symmetry of the group  $2mm$  with the twofold axis along its normal, the full elastic constant matrix reduces to

$$\mathbf{C} = \begin{pmatrix} C_{11} & C_{12} & 0 & 0 & 0 & C_{16} \\ C_{21} & C_{22} & 0 & 0 & 0 & C_{26} \\ 0 & 0 & C_{33} & 0 & 0 & 0 \\ 0 & 0 & 0 & C_{44} & 0 & 0 \\ 0 & 0 & 0 & 0 & C_{55} & 0 \\ C_{61} & C_{62} & 0 & 0 & 0 & C_{66} \end{pmatrix}. \quad (\text{C4})$$

Accordingly, matrix  $\mathbf{A}$  computed by Eq. (B11) is

$$A_{ij} = C_{ij} - \frac{C_{i6}C_{6j}}{C_{66}} \quad i, j = 1, 2, 3. \quad (\text{C5})$$

Using this equation, the coefficients  $A_{11}$ ,  $A_{12}$ , and  $A_{22}$  appearing in Eq. (C3) can be computed from the elastic constants  $C_{ijkl}$  as follows:  $A_{11} = C_{1111} - C_{1133}^2/C_{3333}$ ,  $A_{22} = C_{2222} - C_{2233}^2/C_{3333}$ , and  $A_{12} = C_{1122} - C_{1133}C_{2233}/C_{3333}$ . These ex-

pressions in conjunction with Eq. (C3) will be used in Part II of this work.<sup>5</sup>

### APPENDIX D: STABILITY OF THE FLUID WITH RESPECT TO CRYSTALLIZATION TO A HYDROSTATIC SOLID

In this appendix we give a general proof that a single-component fluid equilibrated with a nonhydrostatically stressed solid composed of the same component tends to crystallize to a hydrostatic solid at the same temperature  $T$  and pressure  $p$ . The proof follows the general line of Gibbs' derivation,<sup>2</sup> which was for a fluid containing at least one more component and thus capable of changing the chemical potential at fixed  $T$  and  $p$ .

We will first revisit Gibbs' famous example with three fluids and point to differences between his multicomponent case and our single-component case. Consider a cubic block of a homogeneous solid whose faces are normal to principal axes of the stress tensor. The principal stresses  $\sigma_{ii}$  are generally different. Suppose the block is immersed in a fluid of the same component and the whole system is in contact with a thermostat. Suppose the solid could be locally equilibrated with the fluid on each face of the cube. Then, the local equilibrium conditions on the separate faces would be

$$u^s - Ts^s + p_i \Omega^s = \mu^f(T, p_i), \quad i = 1, 2, 3, \quad (\text{D1})$$

where  $p_i = -\sigma_{ii}$  are pressures in the fluids. For the multicomponent fluid considered by Gibbs, these three equations could be satisfied with three different chemical potentials adjusted by varying the chemical compositions of the fluids. Thus the solid could be equilibrated with three different fluids. For a single-component fluid, its pressure is the only parameter that could be varied in attempt to satisfy equations Eq. (D1). It is generally impossible to satisfy all three equations for any realistic pressure dependence of  $\mu^f$  at a fixed temperature. Thus, in a single-component system a nonhydrostatic solid cannot be equilibrated with three fluids.

We now proceed to our proof. For a hydrostatically stressed solid, its chemical potential  $\mu_*^s$  is a well-defined quantity that follows the standard relation:<sup>2</sup>

$$u_*^s - Ts_*^s + p \Omega_*^s = \mu_*^s(T, p), \quad (\text{D2})$$

where the asterisk is a reminder that the state is hydrostatic. Subtracting this equation from Eq. (D1) for  $p = p_1$ ,

$$[(u^s - u_*^s) - T(s^s - s_*^s)] + p_1(\Omega^s - \Omega_*^s) = \mu^f(T, p_1) - \mu_*^s(T, p_1). \quad (\text{D3})$$

Note that left-hand side of this equation depends on properties of the solid, the only property of the fluid being its pressure  $p_1$ . Therefore, the sign of the left-hand side can be determined from the following thought experiment. Immerse the same solid in a large container filled with some other fluid medium (e.g., inert gas) which is not soluble in the solid nor is the solid component soluble in that fluid. The fluid has pressure  $p_1$  and the whole system is sealed in a rigid container embedded in a thermostat at temperature  $T$ . Initially, the solid is in a hydrostatic state at pressure  $p_1$  and

thus in mechanical and thermal equilibrium with the fluid. Consider another state in which the solid has the stresses  $\sigma_{ii}$ . It is again in thermal equilibrium with the fluid at temperature  $T$  but obviously not in mechanical equilibrium.

In Eq. (D3), the term in the square brackets is the change in the Helmholtz free energy per atom of the solid upon its deformation at a fixed temperature  $T$  from the initial state to the final. The next term has the meaning of mechanical work done by the solid when displacing the surrounding large mass of the fluid at pressure  $p_1$ . Thus, the left-hand side of Eq. (D3) equals the change (per atom of the solid) in Helmholtz free energy of an isothermal closed system in a rigid

container. Since in the initial state the system is in full equilibrium while in the final state not, this change must be positive. It follows that

$$\mu^f(T, p_1) > \mu_*^s(T, p_1). \quad (\text{D4})$$

Return to the solid in contact with the actual fluid composed on the same component. Equation (D4) shows that the fluid equilibrated with the solid locally at the face with pressure  $p_1$  will tend to crystallize to a hydrostatic solid at the same temperature and pressure. The same is obviously true for two other pressures  $p_2$  and  $p_3$ .

\*tfrolov@gmu.edu

†ymishin@gmu.edu

<sup>1</sup>R. G. Hennig, A. Wadehra, K. P. Driver, W. D. Parker, C. J. Umrigar, and J. W. Wilkins, *Phys. Rev. B* **82**, 014101 (2010).

<sup>2</sup>J. W. Gibbs, *The Collected Works of J. W. Gibbs* (Yale University Press, New Haven, 1948), Vol. 1.

<sup>3</sup>Gibbs (Ref. 2) allowed the solid to contain several chemical elements but assumed its chemical composition to be unvaried. This fixed chemical composition defines the single component of the solid.

<sup>4</sup>R. F. Sekerka and J. W. Cahn, *Acta Mater.* **52**, 1663 (2004).

<sup>5</sup>T. Frolov and Y. Mishin, following paper, *Phys. Rev. B* **82**, 174114 (2010).

<sup>6</sup>S. Balibar, D. O. Edwards, and W. F. Saam, *J. Low Temp. Phys.* **82**, 119 (1991).

<sup>7</sup>R. H. Torii and S. Balibar, *J. Low Temp. Phys.* **89**, 391 (1992).

<sup>8</sup>*Introduction to the Mechanics of a Continuous Medium*, edited by L. E. Malvern (Prentice-Hall, Upper Saddle River, 1969).

<sup>9</sup>J. L. Baum, D. F. Brewer, J. G. Daunt, and D. O. Edwards, *Phys. Rev. Lett.* **3**, 127 (1959).

<sup>10</sup>Y. Huang and G. Chen, *Phys. Rev. B* **72**, 184513 (2005).

<sup>11</sup>E. R. Hernández, A. Rodríguez-Prieto, A. Bergara, and D. Alfè, *Phys. Rev. Lett.* **104**, 185701 (2010).

<sup>12</sup>V. V. Kechin, *J. Phys.: Condens. Matter* **7**, 531 (1995).

<sup>13</sup>M. I. Eremets and I. A. Trojan, *JETP Lett.* **89**, 174 (2009).

<sup>14</sup>A. Lazicki, Y. Fei, and R. J. Hemley, *Solid State Commun.* **150**, 625 (2010).

<sup>15</sup>Y. Mishin, M. J. Mehl, D. A. Papaconstantopoulos, A. F. Voter, and J. D. Kress, *Phys. Rev. B* **63**, 224106 (2001).

<sup>16</sup>*Binary Alloy Phase Diagrams*, edited by T. B. Massalski (ASM, Materials Park, OH, 1986).

<sup>17</sup>J. Morris and X. Song, *J. Chem. Phys.* **116**, 9352 (2002).

<sup>18</sup>F. C. Frank and J. H. van der Merwe, *Proc. R. Soc. London, Ser. A* **198**, 205 (1949).

<sup>19</sup>L. Dong, J. Schnitker, R. W. Smith, and D. J. Srolovitz, *J. Appl. Phys.* **83**, 217 (1998).

<sup>20</sup>J. Li, *Modell. Simul. Mater. Sci. Eng.* **11**, 173 (2003).

<sup>21</sup>F. C. Larché and J. W. Cahn, *Acta Metall.* **33**, 331 (1985).

<sup>22</sup>The fluid components insoluble in the solid can be composed of chemical elements whose concentrations in the solid are negligibly small. As another case, the liquid can be composed of the same elements as the solid but have a different chemical composition. In the latter case, the difference between the composition of the fluid and the fixed composition of the solid can be formally described in terms of additional components insoluble in the solid. When the chemical compositions of the solid and fluid remain equal, the system can be treated as a single-component one.